

Exciton Binding Energy in Semiconducting Single-Walled Carbon Nanotubes

Ying-Zhong Ma,[†] Leonas Valkunas,^{†,‡} Sergei M. Bachilo,[§] and Graham R. Fleming^{*,†}

Department of Chemistry, University of California, Berkeley, and Physical Biosciences Division, Lawrence Berkeley National Laboratory, Berkeley, California 94720-1460; Institute of Physics, Savanoriu Ave. 231, 02300 Vilnius, Lithuania, and Theoretical Physics Department, Faculty of Physics of Vilnius University, Sauletekio Ave. 9, build. 3, 10222 Vilnius, Lithuania; and Department of Chemistry and Center for Biological and Environmental Nanotechnology, Rice University, 6100 Main Street, Houston, Texas 77005

Received: June 6, 2005; In Final Form: July 11, 2005

The exciton binding energy serves as a critical criterion for identification of the nature of elementary excitations (neutral excitons versus a pair of charged carriers) in semiconductor materials. An exciton binding energy of 0.41 eV is determined experimentally for a selected nanotube type, the (8,3) tube, confirming the excitonic nature of the elementary excitations. This determination is made from the energy difference between an electron–hole continuum and its precursor exciton. The electron–hole continuum results from dissociation of excitons following extremely rapid exciton–exciton annihilation and possibly also ultrafast relaxation from the second to the first exciton states and is characterized by distinct spectroscopic and dynamic signatures.

The strong dependence of the spectroscopic and electronic properties of single-walled carbon nanotubes (SWNTs) on their structures provides great promise for a wide range of nanoscale applications.^{1–3} Recent advances in the optical spectroscopy of SWNTs have enabled the connection of the structure with specific spectroscopic characteristics to be established.^{4,5} The variation in the ratio between the energy of the second (E_2) and the first (E_1) electronic transitions for different semiconducting nanotubes^{4,6} from the values predicted by one-electron tight-binding calculations,^{7,8} however, has raised questions about the physical nature of elementary excitations. Following recent theoretical studies,^{9–12} experimental evidence for the presence of excitons has emerged from femtosecond transient absorption (TA) and fluorescence spectroscopic studies.^{13–15} The determination of exciton binding energies for selected tube species was reported very recently, providing strong evidence for the exciton nature of the elementary excitations in semiconducting nanotubes.^{16,17} The observation of photoconductivity in a semiconducting nanotube in response to optical excitation of its E_2 transition, on the other hand, clearly suggests the existence of charged carriers.¹⁸ Photocurrent generation was also observed in electrophoretically deposited SWNT films upon visible excitation.¹⁹

Absorption of a photon with an energy that is equal to or larger than the characteristic band gap of a semiconductor material will create an electron (e) in the conduction band and leave a hole (h) in the valence band. Depending on the magnitude of their Coulombic interaction, the resulting elementary excitation can be either a neutral exciton or a pair of charged carriers (e and h) with weak correlation caused by the Coulombic

interaction.²⁰ A quantity to measure this Coulombic interaction is the exciton binding energy (E_b), defined as the energy difference between the e–h continuum and the corresponding exciton.²¹ If $E_b \gg k_bT$ (thermal energy), then the bound excitons are stable. On the other hand, if E_b is less than or comparable to k_bT , the excitons are not stable and dissociate promptly into charged carriers.²⁰ Quantitative assessment of E_b permits unambiguous identification of the nature of the elementary excitations, a key issue for understanding the physics of semiconducting materials.^{20,21} In this paper, we report an experimental determination of E_b for a selected type of semiconducting SWNT based on femtosecond TA spectroscopy.

The experiment was performed with femtosecond TA spectroscopy with a broadband probe.¹⁴ In brief, the visible and near-infrared (NIR) pump pulses were obtained from the signal and idler outputs of an optical parametric amplifier, pumped by a 250 kHz regeneratively amplified Ti:sapphire system. The pump beam was focused to a spot size of $\sim 300 \mu\text{m}$ at the sample position, and a single-filament white light continuum served as the probe beam. An individual nanotube-enriched sample, prepared by suspending a high-pressure CO-SWNT material in an aqueous solution of sodium dedecyl sulfate micelles, was used.²² Representative TA spectra measured at a delay time of 50 fs for excitation at 953 and 660 nm are shown in Figure 1a. These excitation wavelengths are electronically resonant with the E_1 and E_2 transitions of the (8,3) tube,⁴ enabling selection of this single tube species from a mixture of micelle-dispersed metallic and semiconducting nanotubes. This selection is evident from the TA spectra recorded in the NIR region corresponding to its E_1 transition (Figure 1b,c). In addition to the induced transmission (IT) bands at 660 nm, created by direct optical excitation of the E_2 transition or indirectly via the annihilation of two E_1 excitons,¹⁴ a new IT band peaking at 730 nm is also observed. This band is striking in terms of its ~ 3 times larger amplitude than the 660 nm band in the TA spectrum recorded with the 953 nm pump, and, according to steady-state fluorescence data,⁴

* Corresponding author. E-mail: GRFlemin@lbl.gov. Phone: 510-643-2735. Fax: 510-642-6340.

[†] University of California, Berkeley, and Lawrence Berkeley National Laboratory.

[‡] Institute of Physics and Faculty of Physics of Vilnius University.

[§] Rice University.

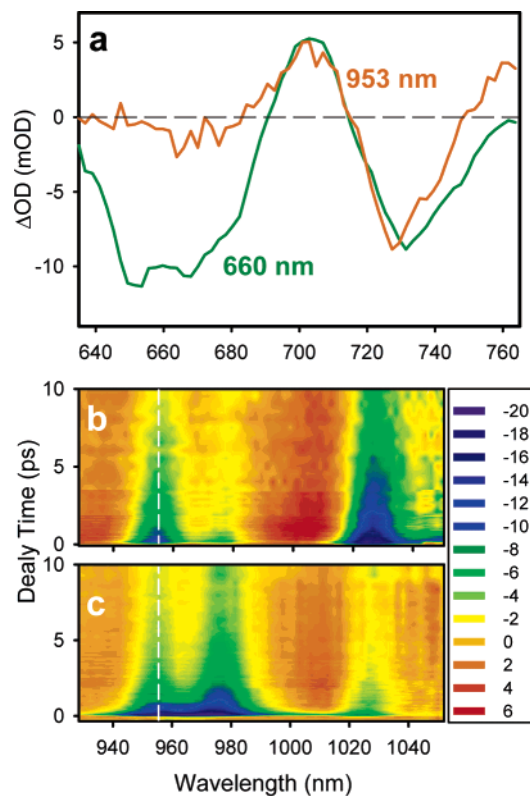


Figure 1. (a) TA spectra measured at a delay time of 50 fs upon excitation at 660 and 953 nm. For ease of comparison, both spectra are scaled to equal amplitude at 730 nm. (b and c) Contour plots of the change of absorbance (in mOD) versus probe wavelength and delay time. The data were recorded upon excitation at (b) 660 and (c) 953 nm. The vertical dashed lines indicate the peak of the induced transmission (IT) bands associated with the E_1 transition of the (8,3) nanotube. The IT bands peaking at 975 and 1026 nm can be assigned to the (6,5) and (7,5) nanotubes, which are simultaneously excited because their E_1 or E_2 transitions fall in the corresponding spectra of pump pulses.

its irrelevance to the (8,3) tube. The similarity of the 730 nm bands obtained with 660 and 953 nm excitation (Figure 1), however, strongly suggests that they are indeed intrinsically related to the (8,3) nanotube. This assignment is further supported by the following facts. (1) Among all other tubes excited via either E_1 or E_2 transitions due to their spectral overlap with the pump pulses,^{4,6} none of them is simultaneously accessible by both 660 and 953 nm pump pulses. (2) A few tube species absorbing around 730 nm such as (8,7), (9,4), and (10,2) can be excited via their strong vibrational subband at $\sim 1550 \text{ cm}^{-1}$ by the 660 nm pump;²³ the accessible tubes accordingly by the 953 nm pump have no absorption peaking at 730 nm.⁶

In view of the multitube contributions to the 730 nm IT band probed with 660 nm excitation, we will focus on the data collected with the E_1 pump. Several distinct differences are found for the kinetics probed at 953 and 730 nm. (1) While the kinetics at 953 nm are invariant with variation of pump intensity (Figure 2a), those at 730 nm exhibit clear pump intensity dependence (Figure 2b). (2) The amplitudes of the 953 nm data scale linearly with the square root of pump intensity, whereas the 730 nm data scale linearly with the intensity itself (Figure 2c). (3) The kinetics obtained at comparable pump intensity show strikingly distinct decay behavior: those obtained at 730 nm are much slower than those at 953 nm (Figure 2d). In contrast to these differences, the time-resolved anisotropies obtained at 730 and 953 nm with resonant E_1 excitation are identical within the experimental uncertainties (Figure 2e).

The dependence of the kinetics detected at 730 nm on the intensity of 953 nm pump pulses (Figure 2b) indicates the occurrence of nonlinear relaxation via a mechanism depending on the nature of elementary excitations. The probable mechanisms include bimolecular exciton–exciton annihilation²⁴ or Auger recombination involving three charged carriers.^{25–27} The population relaxation kinetics of excitons under sufficiently high pump intensity satisfies the following equation:²⁴

$$\frac{dn_{\text{ex}}(t)}{dt} = -\frac{1}{2}\gamma_{\text{ex}}n_{\text{ex}}^2(t) \quad (1)$$

while the kinetics of charged carriers driven by Auger recombination is given by^{25–27}

$$\frac{dn_{\text{eh}}(t)}{dt} = -\frac{1}{3}\gamma_{\text{A}}n_{\text{eh}}^3(t) \quad (2)$$

where $n_{\text{ex}}(t)$ and $n_{\text{eh}}(t)$ are the populations of excitons and charged carriers, respectively, and γ_{ex} and γ_{A} determine the rate constants of the corresponding nonlinear relaxation. The solution of eq 1, $[n_{\text{ex}}(0)/n_{\text{ex}}(t)] - 1 = \gamma_{\text{ex}}n_{\text{ex}}(0)t$, predicts a linear relation between the inverse of the normalized TA signal and delay time (t). The data probed at 730 and 953 nm under the highest pump intensity are plotted in Figure 3a. A linear dependence is clearly evident for the data collected at 953 nm, while the 730 nm data obviously deviate from linearity. This obvious deviation strongly suggests that the new electronic state is not excitonic in nature. In contrast, solution of eq 2 gives the following relationship: $[n_{\text{eh}}(0)/n_{\text{eh}}(t)]^2 - 1 = \gamma_{\text{A}}n_{\text{eh}}^2(0)t$, which coincides with the linear dependence of the 730 nm data in Figure 3b while the 953 nm data clearly do not follow this expression. This result implies that the new state associated with the 730 nm bleaching band is an e–h continuum.^{25–27} In the following, we denote the energy of this new state as E_{eh} .

According to Figure 3 and previous theoretical and experimental work,^{9,10,13,14} we consider both the E_1 and E_2 states as exciton states. As these two states are optically excited in our experiment, creation of an e–h continuum is possible only via dissociation of the excitons. The energy required for this dissociation can be gained via different dynamical processes depending on the exciton state initially excited. For E_1 excitation, the annihilation of two E_1 excitons will create a population in an energetically resonant state (E_n), and the subsequent, rapid relaxation results in branching of the population to the E_2 state¹⁴ and to the E_{eh} state via the dissociation of the hot E_1 excitons formed from E_n to E_1 relaxation. Dissociation of the E_1 exciton may also occur for the E_2 excitation because the rapid $E_2 \rightarrow E_1$ relaxation results in exciton accumulation at the E_1 state and subsequent annihilation.¹³ Furthermore, for direct excitation of the E_2 transition with an intensity that is lower than the threshold of annihilation, the $E_2 \rightarrow E_1$ relaxation itself could produce sufficient excess energy for the resulting E_1 exciton to dissociate provided $E_b \leq E_2 - E_1$. This last scenario is consistent with the observation of photoconductivity in a semiconducting SWNT upon excitation into E_2 .¹⁸ Exciton dissociation involving exciton–exciton annihilation was identified previously in conjugated polymers.²⁸

While the exciton dissociation occurs via different dynamic processes for excitation of the E_2 and E_1 transitions, the resulting e–h continuum originates from the same precursor, the E_1 exciton. Because each exciton state of a SWNT derives primarily from its corresponding e–h band,²⁹ determination of E_b is straightforward when the excitation energies of the E_{eh} and E_1 states are known. These energies are calculated from the peak

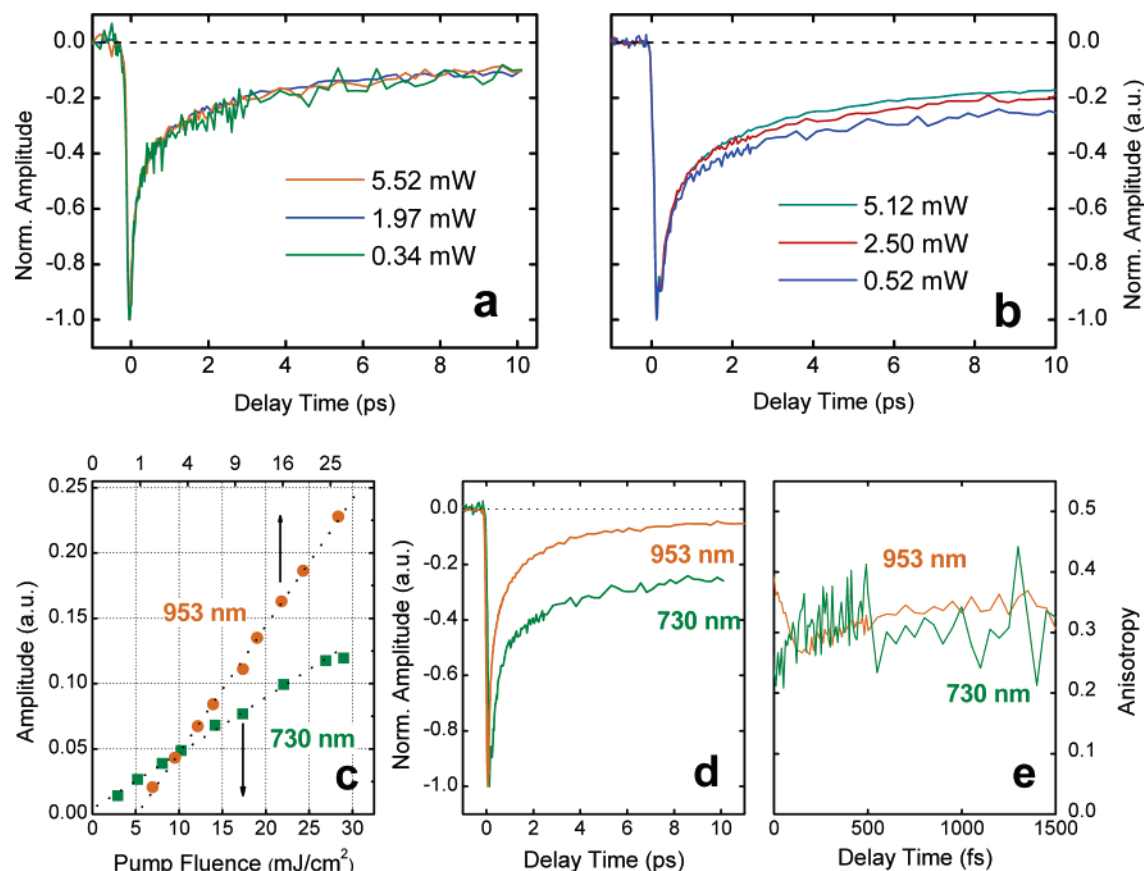


Figure 2. Kinetics probed at (a) 953 and (b) 730 nm under three different 953 nm pump intensities. For ease of comparison, all of the kinetics are normalized at the signal maxima. (c) Dependence of the maximum amplitude of the TA kinetics probed at 730 and 953 nm on the intensity of pump pulses at 953 nm. The two sets of data are plotted separately as a function of the intensity (green vs bottom axis) or its square root (orange vs top axis). The dashed lines are the linear fits to the data. (d) Comparison of the kinetic profile measured at 730 nm under the lowest pump intensity with that obtained at 953 nm. (e) Time-resolved anisotropies at 730 and 953 nm, calculated from $r(t) = [\Delta OD_{\parallel}(t) - \Delta OD_{\perp}(t)] / [\Delta OD_{\parallel}(t) + 2\Delta OD_{\perp}(t)]$ (ΔOD_{\parallel} and ΔOD_{\perp} are respectively the transient absorbances detected at parallel and perpendicular polarization between the pump and probe beams).

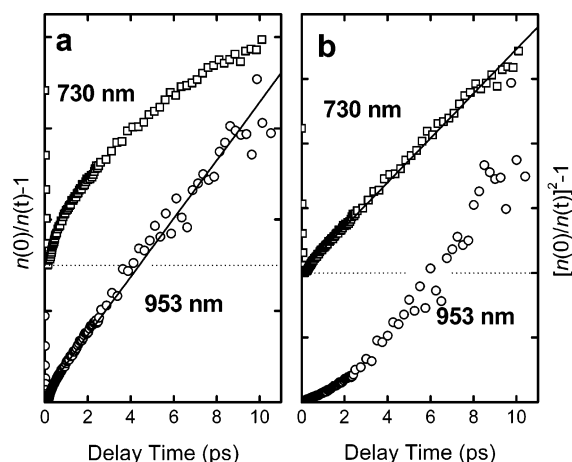


Figure 3. Plot of (a) $[n(0)/n(t)] - 1$ and (b) $[n(0)/n(t)]^2 - 1$ vs time for the data recorded at 730 and 953 nm. See text for details.

positions of the respective IT bands, $E_1 = 1.301$ eV and $E_{eh} = 1.705$ eV, and the E_b value is given by their difference, 0.41 eV for the (8,3) nanotube ($d_t = 7.82$ Å). From the magnitude of E_b , we conclude that the elementary excitations in semiconducting SWNTs are excitons, and the dissociation via the $E_2 \rightarrow E_1$ relaxation is energetically plausible. This value is very close to the experimental results obtained very recently using two-photon excitation spectroscopy.^{16,17} Moreover, this value of E_b falls in the wide range of values calculated using various approaches for SWNTs with a similar diameter to the (8,3) tube,

for example, 0.99 eV from ab initio calculations,^{9,10} 0.53 eV from a semiempirical approach,¹² and 0.40 eV from a variational approach.¹¹ We believe that polaron formation³⁰ and charge stabilization by the ionic wrapping micelles may account for, at least partially, the difference between the theoretical values and our experimentally determined E_b value.

The assignment of the 730 nm IT band to an e–h continuum is strongly supported by the kinetic characteristics shown in Figure 2b–d and additionally by fluorescence excitation data,⁴ as summarized in the following points. (1) The very rapid decay of E_1 excitons via annihilation in comparison to the relatively slow decay of the kinetics at 730 nm (see Figure 2c) creates an initial population $n_{eh}(0)$ in the e–h continuum that is proportional to the annihilation rate of the E_1 excitons, which for direct excitation of E_1 gives a linear intensity dependence.¹⁴ This initial population is needed to solve eq 2 analytically. (2) The different kinetics shown in Figure 2c are intimately tied to the intrinsically different natures of the spectral bands at 953 and 730 nm and to the expected slow reformation of the E_1 excitons from the e–h continuum owing to charge stabilization induced by the net charges on the wrapping micelles and the possible fast formation of long-lived polarons as is observed for conjugated polymers³¹ and organic semiconducting polymers.³² Consequently, the fluorescence emission from the E_1 state upon direct excitation at 730 nm will be diminished, which is consistent with steady-state fluorescence data.⁴ (3) Since the resulting e–h continuum involves the highest valence band and the lowest conduction band, the corresponding band–band transition is,

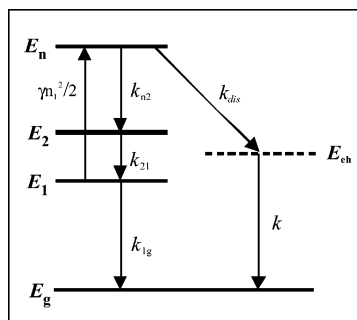


Figure 4. Schematic description of the electronic structure of the (8,3) nanotube and the exciton relaxation pathways. E_g and E_i represent the ground state and the i th exciton state, respectively, and E_{ch} is the e–h continuum. The downward arrows depict the relaxation pathways with corresponding rates as labeled, and the upward arrow denotes the process of populating a higher exciton state as the result of exciton–exciton annihilation.

just like its precursor E_1 exciton, polarized parallel to the tube axis.¹² As a result, the polarization of this continuum remains unchanged, as observed experimentally (Figure 2d).

Additional important support for the assignment of the 730 nm band comes from quantitative comparison of the amplitude ratio between the 953 and 730 nm bands ($\Delta OD_{953}/\Delta OD_{730}$) with the ratio of the oscillator strengths for the transitions into the E_1 and E_{ch} states ($f_{E_1}/f_{E_{ch}}$). A ratio of $\Delta OD_{953}/\Delta OD_{730} \approx 40$ is obtained by direct comparison of the visible and NIR transient absorption spectra and by noting an underestimation from the actual amplitude (by a factor of ~ 2) due to the saturation of the amplitude of the 953 nm signal (see Figure 2c). In the effective mass approximation, the ratio of the oscillator strengths is proportional to the ratio of the length of the nanotube (L) and the exciton radius (r), that is, $f_{E_1}/f_{E_{ch}} \approx L/r$.³³ According to the calculations of refs 9, 10, and 34, r varies with the tube diameter (d_t), and $r = 25$ and 43 Å were obtained for the (8,0) ($d_t = 6.35$ Å) and (7,6) ($d_t = 8.83$ Å) nanotubes, respectively. Assuming $r = 40$ Å for the (8,3) tube ($d_t = 7.82$ Å) and taking $L = 130$ nm,²² we get $f_{E_1}/f_{E_{ch}} \approx 33$, which matches fairly well to the experimental amplitude ratio.

Our observations are summarized in Figure 4. Resonant, moderate to high intensity, excitation of the E_1 and E_2 transitions of the (8,3) nanotube results in exciton dissociation via a secondary process that involves annihilation of the E_1 excitons and possibly the $E_2 \rightarrow E_1$ relaxation for the case of direct excitation of the E_2 transition with an intensity that is lower than the threshold of annihilation. The resulting e–h continuum is located at 1.750 eV and has distinct spectroscopic and dynamical characteristics. On the basis of the excitation energy of this continuum and its precursor exciton, we are able to determine the E_b value as 0.41 eV for the semiconducting (8,3) SWNT. This large E_b value confirms the excitonic nature of the elementary excitations in the semiconducting SWNT. Application of this approach to other semiconducting nanotubes is straightforward and should reveal the relation between the exciton binding energy and nanotube structure. Furthermore, the observation of exciton dissociation allows a natural explanation of the photoconductivity of semiconducting SWNTs.¹⁸ Besides its implications for a deeper understanding of the ultrafast excited-state dynamics and the physical reason for the extremely low quantum efficiency of fluorescence emission, this observation should also serve as a useful guide in the design and optimization of various semiconducting SWNT based electronic elements and devices.

Acknowledgment. The work at Berkeley was supported by the NSF. S.M.B. acknowledges support under NSF CHE-031427

and EEC-0118007. L.V. is thankful for the Fulbright scholarship. We thank S. L. Dexheimer for helpful discussion and R. E. Smalley for providing the HiPco SWNT materials.

References and Notes

- (1) Saito, S.; Dresselhaus, G.; Dresselhaus, M. S. *Physical Properties of Carbon Nanotubes*; Imperial College Press: London, 1998.
- (2) Odom, T. W.; Huang, J.-L.; Kim, P.; Lieber, C. M. *J. Phys. Chem. B* **2000**, *104*, 2794.
- (3) Baughman, R. H.; Zakhidov, A. A.; de Heer, W. A. *Science* **2002**, *297*, 787.
- (4) Bachilo, S. M.; Strano, M. S.; Kittrell, C.; Hauge, R. H.; Smalley, R. E.; Weisman, R. B. *Science* **2002**, *298*, 2361.
- (5) Strano, M. S.; Doorn, S. K.; Haroz, E. H.; Kittrell, C.; Hauge, R. H.; Smalley, R. E. *Nano Lett.* **2003**, *3*, 1091.
- (6) Weisman, R. B.; Bachilo, S. M. *Nano Lett.* **2003**, *3*, 1235.
- (7) Kane, C. L.; Mele, E. J. *Phys. Rev. Lett.* **2003**, *90*, 207401.
- (8) Reich, S.; Maultzsch, J.; Thomsen, C.; Ordejón, P. *Phys. Rev. B* **2002**, *66*, 035412.
- (9) Spataru, C. D.; Ismail-Beigi, S.; Benedict, L. X.; Louie, S. G. *Phys. Rev. Lett.* **2004**, *92*, 077402.
- (10) Spataru, C. D.; Ismail-Beigi, S.; Benedict, L. X.; Louie, S. G. *Appl. Phys. A* **2004**, *78*, 1129.
- (11) Pedersen, T. G. *Phys. Rev. B* **2003**, *67*, 073401.
- (12) Zhao, H.; Mazumdar, S. *Phys. Rev. Lett.* **2004**, *93*, 157402.
- (13) Ma, Y.-Z.; Stenger, J.; Zimmermann, J.; Bachilo, S. M.; Smalley, R. E.; Weisman, R. B.; Fleming, G. R. *J. Chem. Phys.* **2004**, *120*, 3368.
- (14) Ma, Y.-Z.; Valkunas, L.; Dexheimer, S. L.; Bachilo, S. M.; Fleming, G. R. *Phys. Rev. Lett.* **2005**, *94*, 157402.
- (15) Korovyanko, O. J.; Sheng, C.-X.; Vardeny, Z. V.; Dalton, A. B.; Baughman, R. H. *Phys. Rev. Lett.* **2004**, *92*, 017403.
- (16) Wang, F.; Dukovic, G.; Brus, L. E.; Heinz, T. F. *Science* **2005**, *308*, 838.
- (17) Maultzsch, J.; Pomraenke, R.; Reich, S.; Chang, E.; Prezzi, D.; Ruini, A.; Molinari, E.; Strano, M. S.; Thomsen, C.; Lienau, C. *arXiv: cond-mat/0505150* **2005**; <http://arxiv.org/>.
- (18) Freitag, M.; Martin, Y.; Misewich, J. A.; Martel, R.; Avouris, Ph. *Nano Lett.* **2003**, *3*, 1067.
- (19) Barazzouk, S.; Hotchandani, S.; Vinodgopal, K.; Kamat, P. V. *J. Phys. Chem. B* **2004**, *108*, 17015.
- (20) Heeger, A. J. Nature of the primary photoexcitations in poly(arylene-vinylene)s: bound neutral excitons or charged polaron pairs. In *Primary photoexcitations in conjugated polymers: molecular excitation versus semiconductor band model*; Sariciftci, N. S., Ed.; World Scientific: Singapore and River Edge, NJ, 1997; p 20.
- (21) Bäessler, H. Excitons in conjugated polymers. In *Primary photoexcitations in conjugated polymers: molecular excitation versus semiconductor band model*; Sariciftci, N. S., Ed.; World Scientific: Singapore and River Edge, NJ, 1997; p 51.
- (22) O'Connell, M. J.; Bachilo, S. M.; Huffman, C. B.; Moore, V. C.; Strano, M. S.; Haroz, E. H.; Rialon, K. L.; Boul, P. J.; Noon, W. H.; Kittrell, C.; Ma, J.; Hauge, R. H.; Weisman, R. B.; Smalley, R. E. *Science* **2002**, *297*, 593.
- (23) Dresselhaus, M. S.; Eklund, P. C. *Adv. Phys.* **2000**, *49*, 705.
- (24) van Amerongen, H.; Valkunas, L.; van Grondelle, R. *Photosynthetic Excitons*; World Scientific: Singapore, River Edge, NJ, London, and Hong Kong, 2000.
- (25) Ghanassi, M.; Schanne-Klein, M. C.; Hache, F.; Ekimov, A. I.; Ricard, D.; Flytzanis, C. *Appl. Phys. Lett.* **1993**, *62*, 78.
- (26) Klimov, V. I.; Mikhailovsky, A. A.; McBranch, D. W.; Leatherdale, C. A.; Bawendi, M. G. *Science* **2000**, *287*, 1011.
- (27) Htoon, H.; Hollingsworth, J. A.; Dickerson, R.; Klimov, V. I. *Phys. Rev. Lett.* **2003**, *91*, 227401.
- (28) Stevens, M. A.; Silva, C.; Russell, D. M.; Friend, R. H. *Phys. Rev. B* **2001**, *63*, 165213.
- (29) Perebeinos, V.; Tersoff, J.; Avouris, Ph. *Phys. Rev. Lett.* **2004**, *92*, 257402.
- (30) Perebeinos, V.; Tersoff, J.; Avouris, Ph. *Phys. Rev. Lett.* **2005**, *94*, 086802.
- (31) Rothberg, L. Bound polaron pair formation in poly(phenylene-vinylene)s. In *Primary photoexcitations in conjugated polymers: molecular excitation versus semiconductor band model*; Sariciftci, N. S., Ed.; World Scientific: Singapore and River Edge, NJ, 1997; p 129.
- (32) Ruseckas, A.; Gulbinas, V.; Sundström, V.; Undzenas, A.; Valkunas, L. *J. Phys. Chem. B* **1998**, *102*, 7365.
- (33) In the effective mass approximation, f_{E_i} is related to the transition dipole moment of the corresponding band–band transition (p_{eh}) by $f_{E_i} = |p_{eh}|^2 |\varphi_{E_i}(0)|^2$, where $\varphi_{E_i}(\rho)$ is the exciton wave function describing the relative movement of electron and hole separated at a distance of ρ . Taking into account the normalization factors of $\varphi_{E_i}(\rho)$ and the wave function of electrons (holes), it is straightforward to derive $f_{E_i}/f_{E_{ch}} \approx L/r$.
- (34) Pedersen, T. G. *Carbon* **2004**, *42*, 1007.